APPLIED AND ENVIRONMENTAL MICROBIOLOGY, Nov. 1994, p. 4022–4031
0099-2240/94/$04.00+0

Vol. 60, No. 11

Investigation of an Iron-Oxidizing Microbial Mat Community Located near Aarhus, Denmark: Field Studies

DAVID EMERSON[1]* AND NIELS PETER REVSBECH[2]

Center for Microbial Ecology and Department of Microbiology, Michigan State University, East Lansing, Michigan 48824,[1] and Department of Microbial Ecology, University of Aarhus, 8000 Aarhus, Denmark[2]

Received 2 June 1994/Accepted 1 August 1994

We investigated the microbial community that developed at an iron seep where anoxic groundwater containing up to 250 μM Fe^{2+} flowed out of a rock wall and dense, mat-like aggregations of ferric hydroxides formed at the oxic-anoxic interface. In situ analysis with oxygen microelectrodes revealed that the oxygen concentrations in the mat were rarely more than 50% of air saturation and that the oxygen penetration depth was quite variable, ranging from <0.05 cm to several centimeters. The bulk pH of the mat ranged from 7.1 to 7.6. There appeared to be a correlation between the flow rates at different subsites of the mat and the morphotypes of the microorganisms and Fe oxides that developed. In subsites with low flow rates (<2 ml/s), the iron-encrusted sheaths of *Leptothrix ochracea* predominated. Miniature cores revealed that the top few millimeters of the mat consisted primarily of *L. ochracea* sheaths, only about 7% of which contained filaments of cells. Deeper in the mat, large particulate oxides developed, which were often heavily colonized by unicellular bacteria that were made visible by staining with acridine orange. Direct cell counts revealed that the number of bacteria increased from approximately 10^8 to 10^9 cells per cm^3 and the total iron concentration increased from approximately 0.5 to 3 mmol/cm^3 with depth in the mat. Primarily because of the growth of *L. ochracea*, the mat could accrete at rates of up to 3.1 mm/day at these subsites. The iron-encrusted stalks of *Gallionella* spp. prevailed in localized zones of the same low-flow-rate subsites, usually close to where the source water emanated from the wall. These latter zones had the lowest O_2 concentrations (<10% of the ambient concentration), confirming the microaerobic nature of *Gallionella* spp. In subsites with high flow rates (>6 ml/s) particulate Fe oxides were dominant; direct counts revealed that up to 10^9 cells of primarily unicellular bacteria per cm^3 were associated with these particulate oxides. These zones exhibited little vertical stratification in either the number of cells or iron concentration. Finally, mat samples incubated anaerobically in the presence of acetate or succinate exhibited significant potential for iron reduction, suggesting the possibility that a localized iron cycle could occur within the mat community.

When a source of circumneutral-pH, anoxic water that is rich in ferrous iron flows into an oxic zone, it is common for a community of "iron bacteria" to develop at the oxic-anoxic interface and to precipitate ocherous masses of iron hydroxides. These iron seeps are most commonly associated with freshwater wetlands or bogs; however, they may also occur in more-diverse habitats ranging from marine (23) and freshwater (5) hydrothermal vents to the water distribution pipes used for municipal water supplies (34). For a recent review of habitats where microbial interaction with iron and manganese occurs at neutral pH see reference 10.

The bacteria associated with such sites are enigmatic microorganisms because they are difficult to obtain in axenic culture (21, 28, 37). Fortunately, as a result of their copious deposition of Fe oxides, some of them form distinctive metallic casts and can be recognized by their morphotypes in natural samples. Two of the most ubiquitous and unusual morphotypes are those of *Gallionella* spp. and *Leptothrix ochracea*. *Gallionella* spp., which have been obtained in purified cultures, form helical stalks composed primarily of iron oxide with bean-shaped cells attached at the termini (15). *L. ochracea*, one of the most common inhabitants of iron seeps, has not been obtained in pure culture but produces large quantities of condensed ferric iron-encrusted sheaths that appear to be refractile when they are examined with a phase-contrast microscope (37); the sheaths tend to be largely devoid of cells. *Sphaerotilus natans* and *Leptothrix discophora* are heterotrophic, sheathed bacteria that have been obtained in axenic cultures and accumulate iron and ferromanganic oxides, respectively, on their sheaths (9). Workers have also described a number of unicellular bacteria that form capsular layers that become encrusted with iron oxides. Most of these genera are classified in the family *Siderocapsaceae* (16, 18); however, because of the variability in the appearance of the members of these genera and the limited availability of pure cultures, the taxonomic status of these organisms is even more uncertain than the taxonomic status of the stalked and sheathed bacteria.

Although it has been known since the work of Ehrenberg, which was published in 1836 (6), that morphologically distinct microbes may be associated with the deposition of bog iron ore, modern microbiologists have made few systematic attempts to characterize the microbial communities that exist at sites where active iron oxidation and deposition occur at neutral pH. Geochemists have been interested in these sites for a long time as models for understanding the biogeochemical processes that lead to iron or manganese ore deposition. The classic work of Harder (17), a geologist, is still one of the best accounts of the microbiology of these environments. Soil scientists and water distribution experts have initiated studies aimed at identifying the causative agents of biofouling in water distribution pipes (34) and field drains (20). Investigators interested in the early evolution of life and the Earth's

* Corresponding author. Electronic mail address: 22807dem@msu.edu.

atmosphere have studied the fossilized remains of bacteria akin to modern day iron bacteria for hints about the biogeochemistry of the early Earth (19). The quantitative data from most of these reports have focused on the geochemistry and/or age of the Fe oxides, while microbial studies have been primarily phenomenological, describing some of the important morphotypes of the microorganisms present. As a result, very little is known about the fine community structure, the numbers or diversity of the iron bacteria present, and, perhaps most important, the specific role that these organisms play in iron oxidation.

In this report we describe a systematic study of the microbial community at a freshwater iron seep in Denmark. Because of the topology and resultant water flow regimens of this site, the bacteria that inhabit it grow in dense layers that resemble a microbial mat. As a result, it was possible to investigate the community structure and diversity of the characteristic morphotypes of the iron bacteria present, as well as assess the population dynamics of the organisms over the 10 months of this study.

MATERIALS AND METHODS

Site description. The iron seep which we studied was located in the Marselisborg Forest in Aarhus, Denmark (56°N, 10°E). The site consisted of a stone wall (height, 2 m; width, 3 m) built into the bank of a small stream (Fig. 1A). In the middle of the wall was a cement fountain cast in the shape of a lion's head; a metal pipe (diameter, 1.5 cm) formed the lion's mouth, and water flowed from the pipe down into a bowl (30 by 18 by 5 cm), from which it overflowed and dripped down to the stream bank. In addition to the lion's head itself, there were several other sites where water emanated from the rock wall at different flow rates; all of these were characterized by ocherous mats of varying thicknesses. As a result of the varied topologies and flow rates, different flow regimens existed at the site. Our initial observations suggested that the flow regimen influenced the type of mat that developed; thus, five subsites with different flow regimens were chosen for detailed study. The lion's beard (Fig. 1A) was a vertical site between the lion's mouth and the bowl (height, 15 cm; width, 5 to 6 cm), where the water flowed at a rate of <2.0 ml/s and was often entrained in the mat. Water slowly flowed across the bowl itself. The left seep (Fig. 1B) was a shear rock face (height, 1.2 m; width, 7 to 8 cm) where water was always visibly flowing over the surface of the mat at a high rate (>6 ml/s). At the right seep (height, 1.5 m; width, 8 to 10 cm) water flowed at an intermediate rate and varied between being entrained in the mat and flowing over the surface. The final site, the small seep (Fig. 1C), consisted of water trickling out of a crevice in the wall and flowing down about 15 cm to the stream bank; the flow was always entrained in the mat.

General analysis of the mat. For weight determinations, mat material was collected from different subsites, returned to the laboratory, and allowed to stand for approximately 3 h. The overlaying water was decanted, the extraneous leaf material was removed, and the rust-colored mat material, which had the consistency of cottage cheese, was mixed thoroughly. Aliquots (2 ml) of the resulting homogenate were placed in Eppendorf tubes and centrifuged at 8,000 × *g* for 5 min, and the supernatant was removed. The pellets were placed in tared porcelain crucibles and weighed; the net value was taken to be the mat wet weight. The mat material was then dried at 105°C for 24 h and weighed again; the resulting value was taken to be the dry weight. The dried material was burned in a muffle furnace at 550°C for 1.5 h, and the weight of the residue was taken to be the ash weight.

The water temperature in the mat was determined periodically by inserting a thermometer into the top 1 cm of the mat at various points. The pH of the mat was determined by returning samples to the laboratory, mixing them well, and measuring the pH with a standard pH electrode. Water samples collected from the site were analyzed for NO_3^- and NH_4^+ contents with a Technicon II autoanalyzer by standard methods (2, 4). The alkalinity of the water was determined by Gran titration (36).

Core sampling of the mat. Miniature core barrels were made by heating Pasteur pipettes at their shoulders in a propane flame and gently drawing them out to form a tube that, when cut, had a straight barrel that was 15 to 20 mm long and 2.0 to 2.5 mm wide; the wall thickness was 0.2 to 0.3 mm. These core barrels were inserted into the mat by hand and then carefully withdrawn to extract cores up to 10 mm thick. The coring end was sealed with a small plug of modeling clay, and the cores were transported to the laboratory. While being viewed under a stereomicroscope, the cores were extruded onto a microscope slide by gently applying air pressure to the open end of the coring tube. Following extrusion, the intact cores were sectioned with a scalpel at 1-mm intervals. Each section was placed in an Eppendorf tube containing 0.5 ml of deionized water, vortexed, and subsampled to determine acridine orange direct counts of the total number of cells (see below). The remaining sample was stored at −20°C until the total Fe content was determined (see below).

Acridine orange direct counts. A modification of the procedure described by Adams and Ghiorse (1) was used to determine direct counts of bacteria. Acid-washed glass microscope slides were coated on one side with 1% agarose and dried, and then two 1.2-cm-diameter circles were inscribed on each slide with a felt tip pen. The diluted mat sections were vortexed for 30 s, and 10-μl subsamples were spread evenly within the circles and allowed to air dry. A 9-μl portion of deionized water and 1 μl of acridine orange (0.01%, wt/vol) were added directly to each smear, the preparation was mixed, and a coverslip was applied. Counting was done by using the ×100 objective of a Zeiss epifluorescence microscope. Only cell-shaped fluorescent particles were counted; most of these particles were associated either with larger particles of iron hydroxides or with the sheath or stalk material. At least 15 fields per smear were counted, and two smears per core section were examined.

Percentage of ensheathed *L. ochracea* cells. The top 2 mm from a core containing fresh *L. ochracea* sheaths was diluted, such that it was possible to easily distinguish and track individual sheaths when the diluent was spread on a microscope slide. The samples were stained with acridine orange, and random fields containing sheaths were photographed, first under phase-contrast illumination and then under epifluorescent illumination. The resulting prints were used to determine the total length of the sheaths in 24 separate light micrographs (24 microscopic fields) and the total length of fluorescent filaments of cells in the same set of epifluorescent images; dividing the latter number by the former yielded the percentage of sheaths occupied by filaments of cells.

Fe and Mn analysis. The Fe^{2+} concentration in the pore water of the mat was determined in the field by a method similar to that described by Sørensen (32). Water samples were collected with a syringe (5 or 10 ml) and expelled through a 0.22-μm-pore-size syringe filter (Anotec, Banbury, England) into a test tube. A subsample of the filtrate was removed immediately with a pipette and added to a known volume of

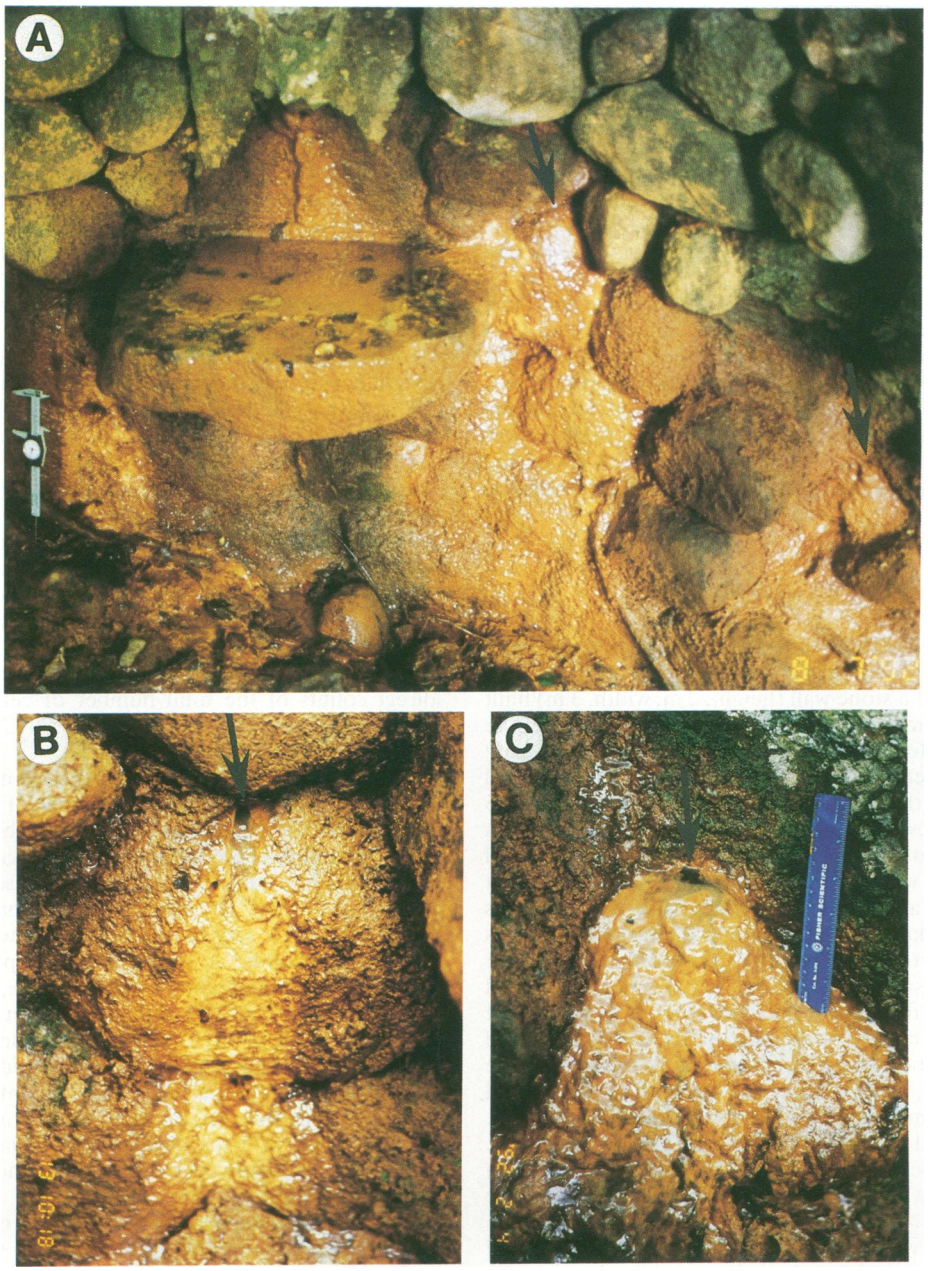

FIG. 1. Marselisborg iron seep. (A) Entire site. The major subsites included the left seep, which is just to the right of the caliper but is partially obscured by the bowl. Just above the bowl is the lion's beard. To the right of the bowl (arrow) is the right seep. At the far right (arrow) is the small seep. (B) Close-up view of the upper portion of the left seep. The arrow indicates the water source. At this subsite the water flowed at a high rate (>6 ml/s) over the surface of the mat, and the depth of the mat was never more than 2 cm. (C) Close-up view of the small seep. The arrow indicates the water source. At this subsite the water trickled slowly and was almost always entrained within the mat. At the time that this photograph was taken, the mat was 7 to 8 cm deep at the midpoint. Note the streaks of greenish oxides within the mat.

ferrozine (36). The samples were returned to the laboratory, and the A_{562} values were determined.

To determine the total Fe content of a core sample, a 50-μl subsample was removed from the diluted core section and placed in 10 ml of a solution containing 0.25 M hydroxylamine and 0.25 M HCl for 1 to 1.5 h in the dark to reduce all of the Fe oxides. A subsample of this material was then diluted into ferrozine, and the absorbance was determined. To determine the free Mn^{2+} concentration, water samples were removed from the bowl, filtered through a 0.22-μm-pore-size filter, and then assayed directly with a flame atomic absorption spectrophotometer (model 370A; Perkin-Elmer). To determine the total Mn concentrations in core samples of the mat, core sections were diluted and reduced with hydroxylamine as described above and then analyzed with the atomic absorption spectrophotometer.

X-ray diffraction studies. Samples of mat material were collected from the small seep and the bowl and mixed together.

A 2- to 3-g (wet weight) portion of the mixture was dried in a desiccator at 21°C for 36 h. An X-ray diffraction analysis was performed at the Geological Institute, University of Aarhus, with a Philips camera, using Cu K-alpha radiation.

Mat accretion rates. The depth of the mat at different subsites was determined at approximately 2- to 3-week intervals by inserting the measuring rod of a caliper into the mat and reading the distance (to the nearest 0.1 mm) when the caliper body just touched the mat surface. An average of three measurements close to each other at each site was used to determine the depth at that site.

Oxygen profiles. Oxygen penetration into the mat was determined in situ with modified Clark-type oxygen microelectrodes containing guard cathodes (29). The microelectrodes had tip diameters of 5 to 10 μm, 90% response times of <2 s, and stirring sensitivities of <2%. The microelectrodes were fitted with an external glass casing that contained silica gel to prevent short circuiting due to moisture buildup in the field (30). The microelectrodes were positioned in the mat with a micromanipulator that was attached to a weighted stand to provide stability. The microelectrodes were first calibrated in the laboratory and then taken to the field, set up, and allowed to polarize for at least 0.5 h prior to use. Calibration in the field was accomplished by using water from a small nearby waterfall to obtain an oxygen-saturated water value; the electrode was then placed in an anoxic section of the mat to obtain the anoxic background current. All current readings were obtained with a battery-operated picoammeter.

Fe reduction. Iron reduction experiments were performed by using a modification of the method described by Lovley and Phillips (25). Samples (several cubic centimeters) of mat material were collected from the left seep and the beard. The excess water was poured off from each sample, extraneous leaves and twigs were removed, and the material was homogenized to a fine paste with a spatula. The resulting material was washed twice with deionized water by centrifugation before being resuspended to its original volume in deionized water. Aliquots (1 g) of the suspension were placed in 100-ml sterile serum vials containing 25 ml of a mineral salts medium (25) supplemented with vitamins (33). Filter-sterilized sodium acetate or sodium succinate was added to each vial to a final concentration of 10 mM, and the vials were gassed with N_2-CO_2 (80:20) and sealed with butyl rubber stoppers. No special effort was made to keep the samples anoxic from the time of collection until they were added to the serum vials. The vials were incubated at 24°C in the dark. Each day subsamples were removed from the vials with a 25-gauge needle and syringe and analyzed for Fe^{2+} content by the ferrozine assay. Control vials contained either no added carbon source, an aerobic atmosphere, or mat material that had been autoclaved at 120°C for 15 min.

RESULTS

Physicochemical properties of the Marselisborg site. The primary source of ferrous iron was the water flowing out of the rock wall. Throughout this study, the Fe^{2+} concentrations at the point sources of water at the different subsites ranged from 150 to 250 μM. It was rare for the Fe^{2+} concentration to be less than 10 μM in any part of the mat; rather, the water at the base of the wall (the point farthest from the source[s]) normally contained two to four times less Fe^{2+} than the source water. Interestingly, the Mn^{2+} concentration in the bulk water collected at the site was also high (around 38 μM).

Since the water flow was over an uneven rock face, the flow volumes were difficult to determine accurately. There was flow at all sites throughout the year, even though the period from May 1992 to July 1992 was one of the driest periods on record for Denmark, with virtually no rainfall. The temperature of the inflowing water varied significantly less (7°C in winter, 12.5°C in summer) than the temperature of the nearby stream (2°C in winter, 18°C in summer). The water contained <1 μM NO_3 and NO_2 and approximately 5 μM NH_4. The alkalinity was around 6 mM, which is typical for groundwaters in this part of Denmark, and as a result the pH of the bulk mat was slightly alkaline, ranging from pH 7.1 to 7.6. In total, these data suggest that the Marselisborg site was supplied with anoxic groundwater rich in Fe(II).

Not surprisingly, a large fraction of the mat was inorganic matter (83% ± 7% of the dry weight averaged over the entire site), and 55% ± 5% of the inorganic material could be recovered as total iron. The X-ray diffraction patterns of the mixed Fe hydroxides collected from the mat revealed no evidence of any crystalline oxides, suggesting that the dominant structural form was amorphous FeOOH. The hydroxides were rapidly reduced by treatment with hydroxylamine or oxalic acid, further suggesting that they were amorphous in nature (3). Close visual inspection of the mat revealed that the subsites with low flow rates were often streaked with veins of a greenish color characteristic of green rusts (Fig. 1C), which result from partial oxidation of Fe(II) under alkaline conditions (32). Subsequent microscopic observations (see below) revealed no qualitative differences in the microbial populations in the green rust zones and the surrounding mat.

Spatial distribution of organisms and Fe oxides. To the naked eye, the texture of the Marselisborg mat appeared to be quite uniform at the different subsites (Fig. 1). Examination of mat material under a microscope, however, revealed significant differences in the appearance of the Fe hydroxides. Furthermore, cursory examination of mat samples by light microscopy revealed an environment nearly devoid of microorganisms; however, when samples were prestained with acridine orange and viewed by epifluorescence microscopy, it was evident that large populations of microorganisms, primarily bacteria, were associated with the Fe oxides (Fig. 2).

Miniature coring profiles revealed both the horizontal fine structure and the vertical fine structure of the mat community. There were three different oxide morphotypes associated with the Marselisborg site: sheaths, stalks, and particulate oxides (Fig. 2). Sheath-bound oxides were almost entirely associated with *L. ochracea* type sheaths (Fig. 2, *L. ochracea* panel), and these structures were predominant at subsites with low flow rates (the lion's beard, the bowl, the small seep) and occurred sporadically in the right seep. Stalk-associated oxides, characteristic of *Gallionella* spp. (Fig. 2, *Gallionella* spp. panel), were found at the same sites, but only in very localized zones, usually near where the source water emanated from the wall. Particulate oxides (Fig. 2, particulate oxides panel) were predominant in the left seep and were often found in the right seep in regions with high flow rates.

The vertical distribution of bacteria as well as iron varied in the mat. In areas dominated by *L. ochracea* type sheaths (Fig. 2, *L. ochracea* panel), the top 1 to 2 mm of the mat consisted of mostly empty, uniform sheaths. A detailed microscopic examination of the top 2 mm of a core taken from the small seep revealed that only about 7% of the sheaths actually contained filaments of rod-shaped cells. Deeper in the mat the sheaths became progressively more encrusted with Fe, and particulate Fe oxides also developed. Most of the microbes present were unicellular and were associated with these particulate oxides; ensheathed cells accounted for less than 5% of the total number of cells at depth. Both the number of cells and

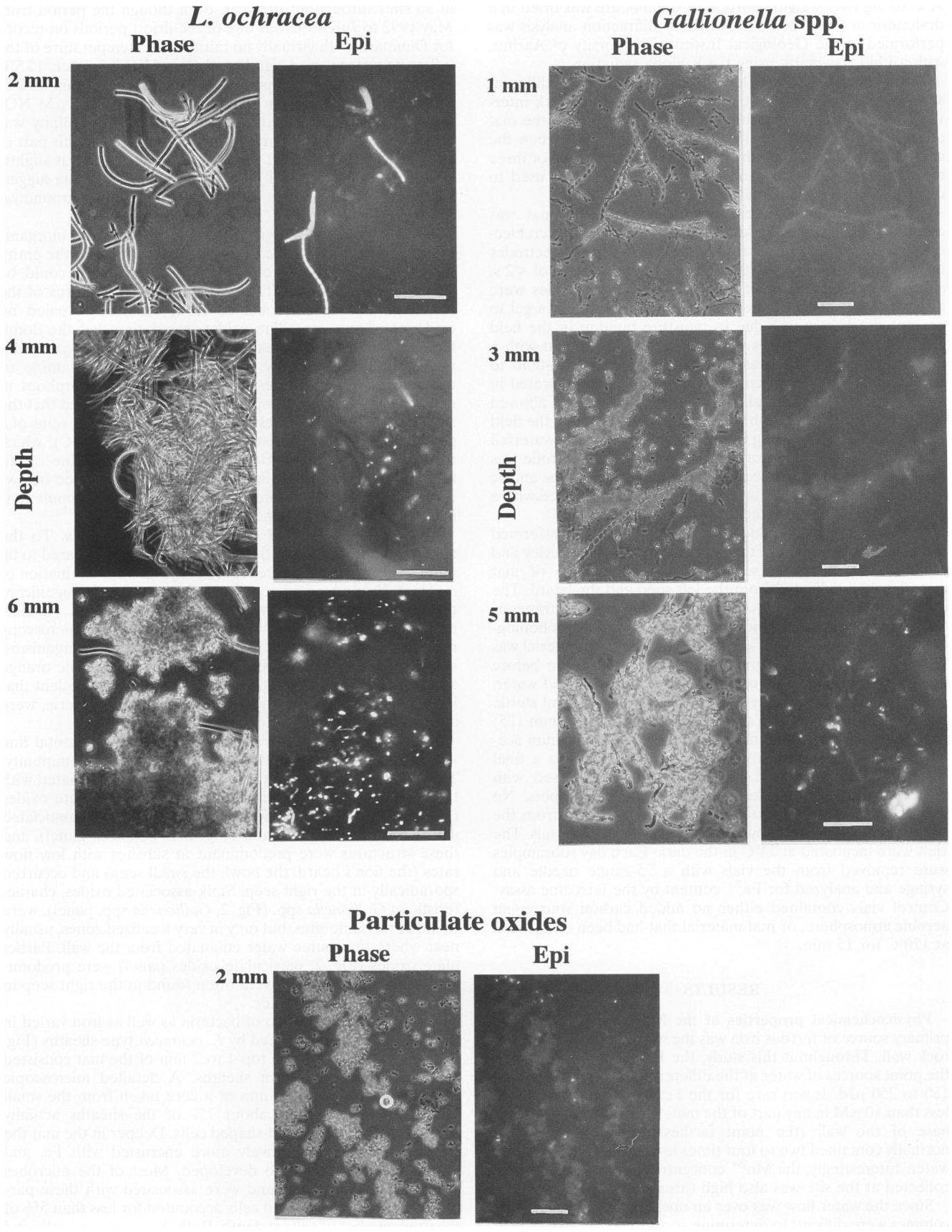
L. ochracea
Phase
Epi
2 mm
4 mm
6 mm
Depth
Gallionella spp.
Phase
Epi
1 mm
3 mm
5 mm
Depth
Particulate oxides
Phase
Epi
2 mm

FIG. 2. Morphology and vertical distribution of microorganisms and Fe oxides at the Marselisborg site as revealed by staining with acridine orange. In each panel the photomicrographs on the left are phase-contrast images, and the photomicrographs on the right are the same images viewed by epifluorescence microscopy, which revealed the acridine orange-stained microbes attached to the oxides. The three panels show typical vertical profiles from cores taken at different subsites in the mat that represent the three morphotypes of iron oxides that occurred (see text for details). *L. ochracea*-type profiles were predominant in the beard, the bowl, and the small seep. *Gallionella*-type profiles occurred within localized zones at these same subsites. Particulate oxide type profiles dominated in the left seep and exhibited little vertical stratification. The sample used for each pair of photomicrographs was diluted approximately 1:200. Bars = 10 μm.

the iron concentration significantly increased with depth in these zones (Fig. 3A).

In regions where *Gallionella* stalks prevailed a similar, although less striking, trend was observed. The top 1 to 2 mm of the mat contained predominantly fresh (i.e., not heavily encrusted) stalk material along with some particulate oxides (Fig. 2, *Gallionella* spp. panel). *Gallionella*-type cells were occasionally seen at the apical ends of the stalks; however, the great majority of cells were associated with the particulate oxides or old stalk material and presumably were not *Gallionella* cells. Deeper in these cores the stalks themselves became heavily encrusted with Fe oxide, and particulate oxides were more abundant and increased in size. At depth, all of the cells were either attached to the old stalk material or associated with the particulate oxides. At these sites there appeared to be a trend toward an increase in the number of cells and Fe concentration in the top 2 to 3 mm of the mat (Fig. 3B).

In the left seep and some regions of the right seep, particulate oxides were dominant (Fig. 2, particulate oxides panel), and remnants of *L. ochracea* sheaths or *Gallionella* stalks were rare. In these zones, the particulate oxides were uniformly distributed throughout the layer, although the size of the individual particles appeared to increase with depth (data not shown). Again, most of the cells were unicellular and associated with these oxides. Unlike the sites containing either sheaths or stalks, the number of cells and Fe concentration remained quite constant with depth in these cores (Fig. 3C).

Oxygen profiles. Oxygen profiles measured in situ revealed that penetration of oxygen into the mat at different sites varied considerably (Fig. 4). In some cases oxygen appeared to be totally depleted within 300 to 400 μm of the mat surface, while in other regions (e.g., the bowl) total depletion of oxygen could not be measured. The oxygen concentrations within 1 to 2 cm of where source water entered the mat were generally lower than the O_2 concentrations in regions downstream (data not shown). Three separate sets of oxygen profiles measured at different times were correlated with regions where *Gallionella* spp. were dominant, and these had the lowest O_2 penetration depths of any of the profiles measured. Two examples of such O_2 profiles from *Gallionella* zones found in the right seep are shown in Fig. 4B and C; in these profiles the O_2 concentrations decreased to below 25 μM, which was less than 10% of the ambient concentration within the top 1 mm of the mat. In contrast, in zones where *L. ochracea* was actively growing, the O_2 concentrations could approach 50% (130 μM) of the ambient concentration (Fig. 4). In the left seep, where particulate oxides predominated (Fig. 4C), the O_2 concentrations were between 20 and 30% of the ambient concentration. Because of the flow-induced turbulent mixing of anoxic source water with air-saturated water at the surface of the mat, oxygen fluxes could not be calculated from these profiles; however, such profiles are illustrative of the variable oxygen dynamics that existed.

Accretion. Both accretion rate and accretion depth varied within different subsites of the mat (Fig. 5). In regions where there was low flow volume and where source water percolated through the mat (e.g., the lion's beard, the bowl, and the small seep), accretion could be extraordinarily rapid; the highest rate measured, 3.1 mm per day, occurred in the lion's beard in August (Fig. 5A). A rate of 2 mm per day was measured during one period in February in the small seep (data not shown).

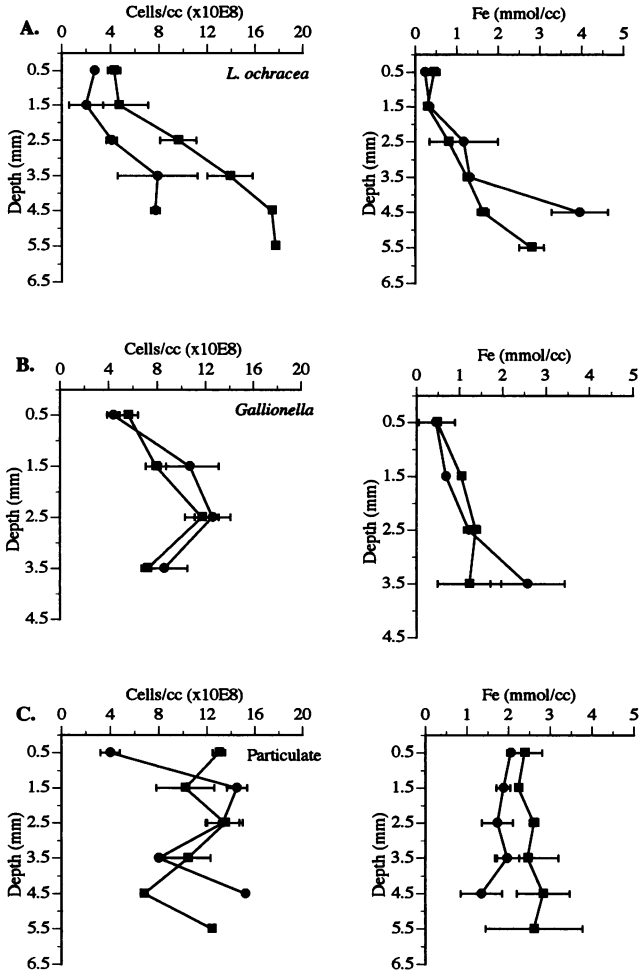

FIG. 3. Vertical profiles of acridine orange direct counts and Fe concentrations in cores that were representative of the different morphotypes of microorganisms and Fe oxides illustrated in Fig. 2. Each line presents data from an individual core that was analyzed for both acridine orange direct counts (left panel) and iron concentrations (right panel). The cores were collected at various times during the study. The error bars indicate ±1 standard deviation from the mean for duplicate samples from the same core. (A) Profiles from zones dominated by *L. ochracea*. Symbols: ●, beard; ■, small seep. (B) Profiles from zones where *Gallionella* stalks were common. Symbols: ● and ■, right seep. (C) Profiles from zones where particulate oxides were dominant. Symbols: ●, left seep; ■, right seep.

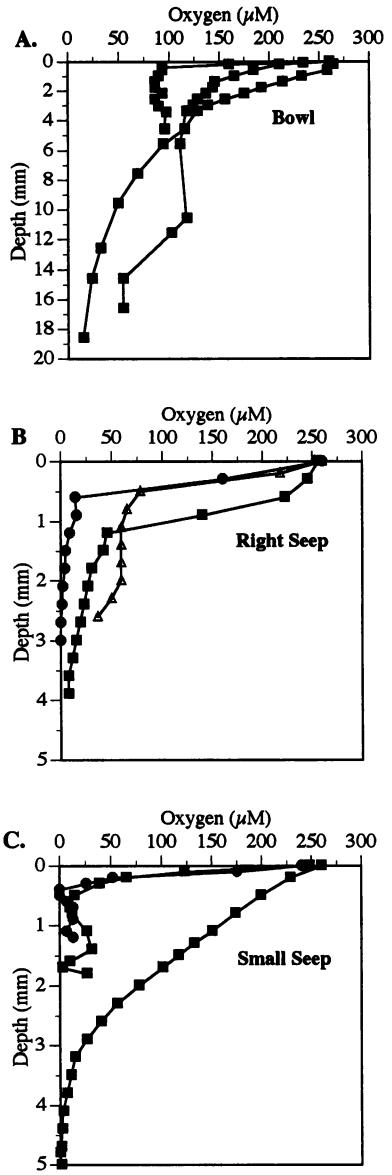

FIG. 4. Oxygen profiles at different subsites of the Marselisborg site. Symbols: ■, O_2 profiles in zones where *L. ochracea* was dominant; ●, profiles where *Gallionella* stalks were found; △, profiles where particulate oxides were dominant. The profiles were measured at different times during the study. (A) Bowl. Note that the *y* axis for panel A is different from the *y* axis for panels B and C. (B) Right seep. In the right seep all three morphotypes occurred. The profile obtained where *Gallionella* spp. were present near the source water inlet exhibited the most rapid depletion of O_2. (C) Small seep. Two of the small seep profiles indicate that in some regions the difference in O_2 concentration between zones dominated by *L. ochracea* and zones dominated by *Gallionella* spp. could be quite small.

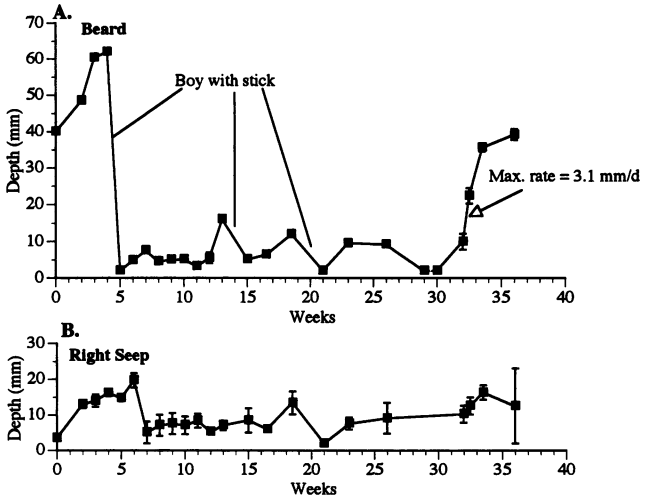

FIG. 5. Accretion of the mat at two subsites. Each datum point is the mean of three measurements; the error bars (not always visible) indicate ±1 standard deviation from the mean. At the beard subsite several times human intervention caused nearly complete removal of the mat. The maximum rate of accretion, 3.1 mm per day, was measured in August 1992. At the right seep, probably because of the high water flow rate, the mat never reached a depth of more than 20 mm; however, a similar pattern was observed where mat accretion followed by sloughing off was evident.

Human intervention often caused nearly complete removal of the mat from the wall (Fig. 5A) and the bowl; however, it always grew back again, although there could be lag periods of 2 to 4 weeks before reestablishment began. When nature was allowed to take its course at the vertical sites with low flow rates (the beard and the small seep), the mat accreted to a depth of several centimeters before gravity prevailed and the bulk of the mat sloughed off. At the high-flow-rate sites, the mat accreted more slowly, and it never reached a depth of more than 20 mm in the right seep (Fig. 5B) and 15 mm in the left seep. This was probably due to the mechanical shear caused by the high water flow rates at these subsites.

Accretion of the mat appeared to require a flow of iron-rich water. In a section of the small seep where the water flow was terminated because of topological changes in the mat, accretion stopped and the mat shrank slowly over a 1-month period. During the same period, the adjacent mat, which received water flow, accreted over 1 cm (data not shown).

Fe reduction. Samples of mat material incubated anaerobically with acetate or succinate exhibited appreciable rates of reduction of the native oxides, indicating that there was a population of Fe^{3+}-reducing bacteria in the mat (Fig. 6). When a magnet was placed on a serum bottle in which reduction had occurred, no magnetic particles were attracted to it. This suggested that magnetite was not a product of the reduction, which may have reflected the form of the naturally occurring amorphous oxides. Samples that were heat sterilized before carbon sources were added exhibited little or no reduction (Fig. 6), and samples that were not amended with a carbon source or that contained a carbon source but were incubated aerobically also did not exhibit reduction (data not shown).

DISCUSSION

The Marselisborg site offered an unusual opportunity to study an environment dominated by iron bacteria at near neutral pH. Often iron seeps are found in streams or wetlands where the bacteria grow as relatively diffuse flocs in slowly flowing water containing Fe(II). Because these flocs lack density, disperse easily, and are subjected to mixing, it is often difficult to assess their population dynamics or heterogeneity. Because of the topology and water flow patterns at the

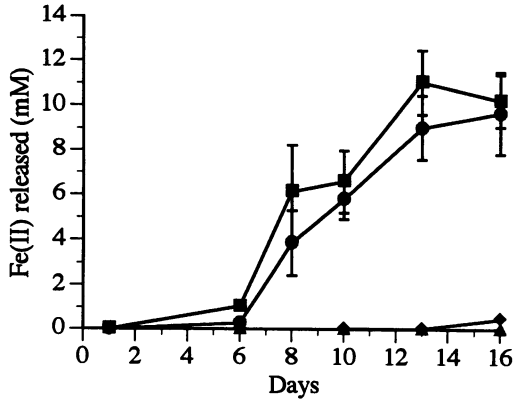

FIG. 6. Fe reduction potential. Samples of mat material were incubated anaerobically in the presence of 10 mM acetate (■) or 10 mM succinate (●), and the amount of Fe^{2+} released was determined by the ferrozine assay. Each point is the mean of three determinations; the error bars indicate ±1 standard deviation from the mean. Heat-sterilized controls containing acetate (◆) or succinate (▲) were also included in the experiment.

Marselisborg site, the Fe oxides and the bacteria associated with them occurred in dense aggregations that could be sampled nearly intact so that natural stratification of the population could be studied in detail. Two striking features of this mat were (i) the tremendous masses of ocherous deposits that developed in short time periods and (ii) the fact most of the bacteria (up to 10^9 cells per cm^3) appeared to be tightly associated with the Fe oxides and were visible only when they were stained with acridine orange and viewed by epifluorescence microscopy.

The flow rate of Fe^{2+}-rich water appeared to be a key determinant of the oxide morphotype, the type of cell population, and the accretion rate in a given region of the Marselisborg mat. To summarize, in sites where the water flowed actively over the surface of the mat at a high rate (e.g., the left seep), net accretion was slow and particulate oxides that had unicellular microbes associated with them were predominant; there was little vertical stratification of cells or Fe. The sites where most of the water flow was entrained in the mat (e.g., the beard and the small seep) had the most rapid net accretion rates. These sites, especially those dominated by *L. ochracea*, exhibited significant vertical stratification of the number of cells and morphotype, as well as Fe concentration. In the right seep, where both high and medium flow regimens occurred, all three morphotypes of cell-associated Fe oxides were present. If the flow ceased, the mat remained static or even shrank slowly.

The development of the mat did not seem to be affected seasonally. Quantitative core samples were taken in January, March, May, July, and September of 1992, and qualitative samples were obtained every 3 to 4 weeks during this period. While there were significant changes in overall depth and accretion rate in the mat at the different subsites during this time, the trends for individual core profiles, as reported above, were much the same. This constancy probably reflects the relatively stable temperature and Fe^{2+} concentration of the water.

The role of Mn and manganic oxides at the Marselisborg site also deserves some mention. The total Mn concentrations in core samples of the mat were determined twice, once in late spring and once in summer. In both instances we found significant concentrations of Mn, presumably mostly in the Mn(IV) state. At the left seep, the total Mn concentrations ranged from 0.2 to 0.4 $mmol/cm^3$, values which were about 10 to 20% of the total iron concentration values for the same cores. A core from an *L. ochracea* type zone in the small seep had detectable Mn concentrations (0.1 to 0.2 $mmol/cm^3$). These results indicate that Mn oxidation occurred in the mat and that ferromanganic oxides probably were present in significant amounts; however, more work is needed to clarify the role of Mn and its interaction with Fe within the mat.

L. ochracea appeared to be a key mat-building organism, since it was commonly associated with the most rapidly accreting parts of the mat in the subsites with low flow rates. On the basis of our results, a model for accretion of the mat by *L. ochracea* can be postulated. Presumably, *L. ochracea* cells attach to substrata on the rock wall and begin growing out from the surface. As the cells grow, they maintain their most active growth zone at the top of the mat in the presence of the highest concentrations of Fe^{2+} and O_2 and leave behind a copious matrix of vacated, tubular sheath material coated with fine-grain Fe oxides. Immediately below this growth zone, the vacated sheaths appear to serve as a substrate for further iron oxidation and become more heavily encrusted with Fe oxides. The exterior surfaces of these aged, empty sheaths also serve as attachment sites for unicellular bacteria, which in turn also become encrusted with Fe oxides. In these deeper regions, particulate Fe oxides also begin to form, and these oxides may harbor high densities of unicellular bacteria. These particles are often associated with empty sheaths, but whether the sheaths actually serve as nucleation centers for their formation is not known. As the mat matrix grows outward, it begins to entrain more water in the mat. The flow path of the water entrained in the mat has greater tortuosity, which results in a decrease in the water velocity. A reduction in velocity results in a decrease in the drag forces on the sheath filaments created by the flowing water, which allows the cell filaments to grow longer without being sheared off. Ultimately, this habitat modification provides a more hospitable environment for the growth and further accretion of filamentous bacteria and ultimately for accumulation of unicellular bacteria on the empty sheaths and particulate oxides that develop deeper in the mat.

The presence of *Gallionella* stalks was sporadic and very localized in the regions where *L. ochracea* grew; however, where stalks were abundant, it appeared that they formed the dominant substratum of the mat. In numerous samples members of these two genera were never observed to coexist in the top 2 mm of the mat, where most of the viable cells of these organisms were observed. In one case, samples taken less than 1 cm apart in the small seep were completely distinct with respect to the two morphotypes. Occasionally, in deeper cores a zone that was dominated by *L. ochracea* on the surface had significant numbers of stalks (devoid of apical cells) at depth, suggesting that at some time *Gallionella* spp. may have dominated at the same location. However, a note of caution concerning the presence of *Gallionella* spp. in the mat is necessary; recent studies have shown that under some conditions *Gallionella ferruginea* may not form stalks and grows unicellularly (12, 14). In such cases it would be difficult to distinguish *G. ferruginea* from the numerically dominant non-appendaged unicellular bacteria found in the mat (see below). In addition, the vortexing necessary to disperse the cells for counting may have caused some separation of apical cells from the stalks. Phylogenetic probes could provide an excellent tool for resolving these dilemmas.

Although the occurrence of *Gallionella* spp. was sporadic, when *Gallionella* cells were found, they were usually within a

few centimeters of locations where water was emanating from the wall. As oxygen microelectrode studies showed, these areas were also the areas where the oxygen concentrations were lowest (<10% of the ambient concentration). These results suggest that oxygen might be an important factor controlling which of the two organisms (*Gallionella* spp. or *L. ochracea*) colonizes a specific region of the mat, although the possibility that there are additional unknown nutritional factors cannot be ruled out. Laboratory cultures of *Gallionella* spp. have shown that these organisms are microaerophiles that normally grow at oxygen concentrations that are equivalent to less than 1% of the ambient saturation (15). On the other hand, it has been speculated that *L. ochracea* also prefers to grow in the presence of very low oxygen tensions (27). However, our microelectrode studies revealed that *L. ochracea* was often found in more oxygenated regions of the mat; for example, large blooms of *L. ochracea* were common in the bowl, where the oxygen concentrations approached 50% of air saturation. Thus, *L. ochracea* is probably not a true microaerophile.

The role of the numerically dominant unicellular bacteria associated with the particulate oxides is intriguing. Without obtaining axenic cultures and/or using phylogenetic probes for the dominant members of the unicellular consortia, it is not possible to determine the diversity of this population, nor is it possible to determine whether the unicellular bacteria found in low- and high-flow-rate subsites are the same. Light microscopy revealed that these particle-associated microbes had a variety of morphotypes, suggesting that they probably are members of diverse taxa. In any case, these unicellular microbes may be similar to members of the family *Siderocapsaceae*. These poorly characterized organisms are phenotypically defined as organisms that produce Fe-encrusted capsules (16, 18). The dense aggregates which the particulate oxides formed probably offered them an advantage in resisting the drag and shearing forces of the water flowing over the wall, especially in vertical subsites with high flow rates.

The close physical association of the bacteria and the Fe oxides, the correlation between increases in iron concentration and increases in the number of cells, and the dependence for accretion of the mat on the Fe^{2+}-rich water suggest that the bacteria actively mediate the oxidation of iron, if they do not use it directly as an electron donor. For a long time *G. ferruginea* has been considered a lithotroph (17), although this contention has been based largely on circumstantial evidence (22). Recent data, however, suggest that *G. ferruginea* is capable of autotrophic growth by using Fe^{2+} as an energy source (13, 14). The case for lithotrophic growth of *L. ochracea* is even more equivocal, since purified cultures of this organism are not available. Perhaps the most interesting question in this regard concerns the role of the numerically dominant, unicellular bacteria associated with the particulate oxides and whether they mediate the oxidation of Fe(II) to Fe(III) and couple it to energy production.

Laboratory studies carried out with samples from the mat showed that microbes from the mat were responsible for up to 80% of the Fe oxidation; furthermore, this process was inhibited by azide (8). Since these experiments were carried out with natural enrichment cultures, it was not possible to determine specifically which morphological type(s) of organisms was responsible, although unicellular microbes, not *L. ochracea* and *Gallionella* spp., were numerically dominant. An alternative explanation, however, is that the bacteria are simply entrapped in the oxide matrix. It has been shown that amorphous Fe oxides can act as an efficient ion-exchange matrix to bind microbial cells (26). In this passive oxidation scenario, lipopolysaccharides or anionic capsular layers on the cell surface could bind additional Fe^{2+}, which would then chemically oxidize and encapsulate the bacteria in an iron oxide matrix. Of course, it is quite possible that active and passive iron oxidation processes occur simultaneously in the mat.

Interestingly, other well-known iron bacteria, such as *S. natans* and *L. discophora*, did not appear to be common inhabitants at the Marselisborg site. It may not be surprising that *S. natans* was not present since this organism is known to prefer eutrophic habitats (9); however, *L. discophora* is commonly found in low-nutrient environments. The characteristic fluffy sheaths of *L. discophora* were rarely seen in numerous observations by light microscopy, and enrichment (7) for this organism did not yield any isolates. Apparently this heterotrophic Mn- and Fe-oxidizing bacterium was not able to compete under the conditions that existed at the Marselisborg site. In addition, representatives of the heterotrophic budding bacteria, such as *Pedomicrobium* and *Hyphomicrobium* species, which are known to produce Fe-encrusted capsules (11), were not commonly observed to be a part of the microbial community.

The potential rates of Fe reduction which we observed in the mat are among the highest rates reported for an unenriched, natural population (24). This is probably due to two factors: (i) a significant population of microbes with the metabolic capacity to reduce iron must exist in the mat, and (ii) the amorphous oxides formed within the mat are ideal substrates for Fe-reducing bacteria. These results suggest that if a suitable electron donor (e.g., acetate) is present, dissimilatory iron reduction could occur in anoxic zones of the mat. The Fe^{2+} released could be oxidized by the bacteria in the upper, aerobic regions of the mat, thereby creating a localized iron cycle within the mat itself.

ACKNOWLEDGMENTS

We thank Lars Pedersen for technical assistance. We are also indebted to Bo Thamdrup and Jens W. Hansen for help with X-ray diffraction and Mn analyses, respectively, as well as many helpful discussions during the study.

This work took place while D.E. participated in a scholar exchange program between the Danish Center for Microbial Ecology and the Center for Microbial Ecology at Michigan State University. The work at the University of Aarhus was supported by the Danish Center for Microbial Ecology; work at Michigan State University was supported by National Science Foundation grant BIR9120006.

REFERENCES

1. **Adams, L. F., and W. C. Ghiorse.** 1985. Influence of manganese on growth of a sheathless strain of *Leptothrix discophora*. Appl. Environ. Microbiol. **49**:556–562.
2. **Armstrong, F. A., C. R. Stearns, and J. D. Strickland.** 1967. The measurement of upwelling and subsequent biological processes by means of the Technicon autoanalyzer and associated equipment. Deep-Sea Res. **14**:381–389.
3. **Borgaard, O. K.** 1988. Phase identification by selective dissolution techniques, p. 83–98. *In* J. W. Stucki et al. (ed.), Iron in soils and clay minerals. D. Reidel Publishing Co., Boston.
4. **Bower, C. E., and T. Holm-Hansen.** 1980. A salicylate-hypochlorite method for determining ammonia in seawater. Can. J. Fish. Aquat. Sci. **37**:794–798.
5. **Dymond, J., R. W. Collier, and M. E. Watwood.** 1989. Bacterial mats from Crater Lake, Oregon and their relationship to possible deep-lake hydrothermal venting. Nature (London) **342**:673–675.
6. **Ehrenberg, C. G.** 1836. Vorlage Mittheilungen ueber das wirklige Vorkommen fossiler Infusiorien und ihre grosse Verbreitung. Poggendorff's Ann. **38**:213–227.
7. **Emerson, D., and W. C. Ghiorse.** 1992. Isolation, cultural maintenance, and taxonomy of a sheath-forming strain of *Leptothrix discophora* and characterization of manganese-oxidizing activity associated with the sheath. Appl. Environ. Microbiol. **58**:4001–4010.

8. **Emerson, D., and N. P. Revsbech.** 1994. Investigation of an iron-oxidizing microbial mat community located near Aarhus, Denmark: laboratory studies. Appl. Environ. Microbiol. **60:**4032–4038.
9. **Ghiorse, W. C.** 1984. Biology of iron- and manganese-depositing bacteria. Annu. Rev. Microbiol. **38:**515–550.
10. **Ghiorse, W. C., and H. L. Ehrlich.** 1993. Microbial biomineralization of iron and manganese, p. 75–99. *In* R. W. Fitzpatrick and H. C. W. Skinner (ed.), Iron and manganese biomineralization processes in modern and ancient environments. Catena, Cremlingen-Destedt, Germany.
11. **Ghiorse, W. C., and P. Hirsch.** 1979. An ultrastructural study of iron and manganese deposition associated with extracellular polymers of *Pedomicrobium*-like budding bacteria. Arch. Microbiol. **123:**213–226.
12. **Hallbeck, L., and K. Pedersen.** 1990. Culture parameters regulating stalk formation and growth rate of *Gallionella ferruginea*. J. Gen. Microbiol. **136:**1675–1680.
13. **Hallbeck, L., and K. Pedersen.** 1991. Autotrophic and mixotrophic growth of *Gallionella ferruginea*. J. Gen. Microbiol. **137:**2657–2661.
14. **Hallbeck, L., F. Ståhl, and K. Pedersen.** 1993. Phylogeny and phenotypic characterization of the stalk-forming and iron-oxidizing bacterium *Gallionella ferruginea*. J. Gen. Microbiol. **139:**1531–1535.
15. **Hanert, H. H.** 1992. The genus *Gallionella*, p. 4082–4088. *In* A. Balows, H. G. Trüper, M. Dworkin, W. Harder, and K. H. Schliefer (ed.), The prokaryotes, 2nd ed., vol. 4. Springer-Verlag, New York.
16. **Hanert, H. H.** 1992. The Genus *Siderocapsa* (and other iron- or manganese-oxidizing eubacteria), p. 4102–4113. *In* A. Balows, H. G. Trüper, M. Dworkin, W. Harder, and K. H. Schliefer (ed.), The prokaryotes, 2nd ed., vol. 4. Springer-Verlag, New York.
17. **Harder, E. C.** 1919. Iron-depositing bacteria and their geologic relations. U. S. Geol. Surv. Professional Papers **113:**7–89.
18. **Hirsch, P., G. A. Zavarzin, and O. H. Tuovinen.** 1992. Genus I. "*Siderocapsa*," p. 1875–1878. *In* J. T. Staley, M. P. Bryant, N. Pfennig, and J. G. Holt (ed.), Bergey's manual of systematic bacteriology, vol. 3. Williams and Wilkins, Baltimore.
19. **Horodyski, R. J., and L. P. Knauth.** 1994. Life on land in the Precambrian. Science **263:**494–498.
20. **Ivarson, K. C., and M. Sojak.** 1978. Microorganisms and ochre deposits in field drains of Ontario. Can. J. Soil Sci. **58:**1–17.
21. **Jones, J. G.** 1986. Iron transformations by freshwater bacteria. Adv. Microb. Ecol. **9:**149–185.
22. **Jørgensen, B. B.** 1989. Biogeochemistry of chemoautotrophic bacteria, p. 117–146. *In* H. G. Schlegel and B. Bowien (ed.), Autotrophic bacteria. Science Tech Publishers and Springer-Verlag, Madison, Wis.
23. **Karl, D. M., G. M. McMurtry, G. M. Malahoff, and M. O. Garcia.** 1988. Loihi seamount, Hawaii: a mid-plate volcano with a distinctive hydrothermal system. Nature (London) **335:**532–535.
24. **Lovley, D. R.** 1991. Dissimilatory Fe(III) and Mn(IV) reduction. Microbiol. Rev. **55:**259–287.
25. **Lovley, D. R., and E. J. P. Phillips.** 1986. Organic matter mineralization with reduction of ferric iron in anaerobic sediments. Appl. Environ. Microbiol. **51:**683–689.
26. **Macrae, I. C., and J. F. Edwards.** 1972. Adsorption of colloidal iron by bacteria. Appl. Microbiol. **24:**819–823.
27. **Mulder, E. G., and M. H. Deinema.** 1992. The sheathed bacteria, p. 2612–2624. *In* A. Balows, H. G. Trüper, M. Dworkin, W. Harder, and K. H. Schliefer (ed.), The prokaryotes, 2nd ed., vol. 4. Springer-Verlag, New York.
28. **Nealson, K. H.** 1983. The microbial iron cycle, p. 159–190. *In* W. Krumbein (ed.), Microbial geochemistry. Blackwell Scientific, Boston.
29. **Revsbech, N. P.** 1989. An oxygen microelectrode with a guard cathode. Limnol. Oceangr. **34:**474–478.
30. **Revsbech, N. P., and B. B. Jørgensen.** 1986. Microelectrodes: their use in microbial ecology. Adv. Microb. Ecol. **9:**293–353.
31. **Schwertmann, U., and R. M. Cornell.** 1991. Iron oxides in the laboratory, p. 119–121. VCH Publishers, New York.
32. **Sørensen, J.** 1982. Reduction of ferric iron in anaerobic, marine sediment and interaction with reduction of nitrate and sulfate. Appl. Environ. Microbiol. **43:**319–324.
33. **Staley, J. T.** 1968. *Prosthecomicrobium* and *Ancalomicrobium*: new prosthecate freshwater bacteria. J. Bacteriol. **95:**1921–1942.
34. **Starkey, R. L.** 1945. Transformations of iron by bacteria in water. J. Am. Water Works Assoc. **37:**963–984.
35. **Stookey, L. L.** 1970. Ferrozine—a new spectrophotometric reagent for iron. Anal. Chem. **42:**779–781.
36. **Talling, J. F.** 1973. The application of some electrochemical methods to the measurement of photosynthesis and respiration in fresh waters. Freshwater Biol. **3:**335–362.
37. **van Veen, W. L., E. G. Mulder, and M. H. Deinema.** 1978. The *Sphaerotilus-Leptothrix* group of bacteria. Microbiol. Rev. **42:**329–356.